We are IntechOpen,
the world's leading publisher of
Open Access books
Built by scientists, for scientists

6,400
Open access books available

174,000
International authors and editors

190M
Downloads

Our authors are among the

154
Countries delivered to

TOP 1%
most cited scientists

12.2%
Contributors from top 500 universities

BOOK CITATION INDEX
CLARIVATE ANALYTICS
INDEXED

WEB OF SCIENCE™

Selection of our books indexed in the Book Citation Index
in Web of Science™ Core Collection (BKCI)

Interested in publishing with us?
Contact book.department@intechopen.com

Numbers displayed above are based on latest data collected.
For more information visit www.intechopen.com

Chapter

Optimised PVDF Placement Inside an Operating Hydrodynamic Thrust Bearing

*Andrew Youssef, David Matthews, Andrew Guzzomi and Jie Pan*

Abstract

In our previous work we demonstrated the feasibility of using Polyvinylidene Fluoride (PVDF) sensors inside an operational thrust bearing and were able to measure the blade passing frequencies (BPF) due to an asymmetric flow around different propellers. In that work however the sensors were positioned inside the flat surface of the stationary portion of the bearing with the tilted pads rotated on the opposite side. Due to this configuration the output signal of the PVDF consisted of a superposition of the pad passing frequency (PPF) and the blade passing frequency (BPF) making it difficult to extract useful information from the results. Here, an improved bearing pad-film configuration is proposed in order to minimise the effects of the PPF. By embedding the films inside the pads, positioned on the stationary side of bearing, and rotating the flat surface, it was possible to eliminate the PPF and significantly increase the signal to noise ratio. The measured results give a better understanding of the fundamental vibratory components that arise from the propeller-shaft system.

Keywords: PVDF, monitoring, thrust bearing, force transducer, marine vessels, piezoelectric sensor

1. Introduction

Most marine vessels have propellers at the stern operating in non-linear wakes. This propeller placement is done primarily for ease of construction and propulsion efficiency. The main disadvantage of such a setup is having to operate in a region where the wake is non-linear. This generates noise from an oscillating thrust and, in terms of hull induced vibrations at frequencies below 100 Hz [1], can have large effects on passenger comfort, mechanical wear and acoustic detection. Developing an accurate vibrational model of the propulsion system in a non-uniform wake is extremely difficult. It is necessary to have a good understanding of the hydrodynamic forces inside the thrust bearing and measuring this force is logistically difficult. This is due to the complex nature of thrust bearings which self stabilise based on operating parameters such as speed and load [2]. To simplify the inclusion of thrust bearing stiffness in analytical modelling, simple linear stiffness representations are used
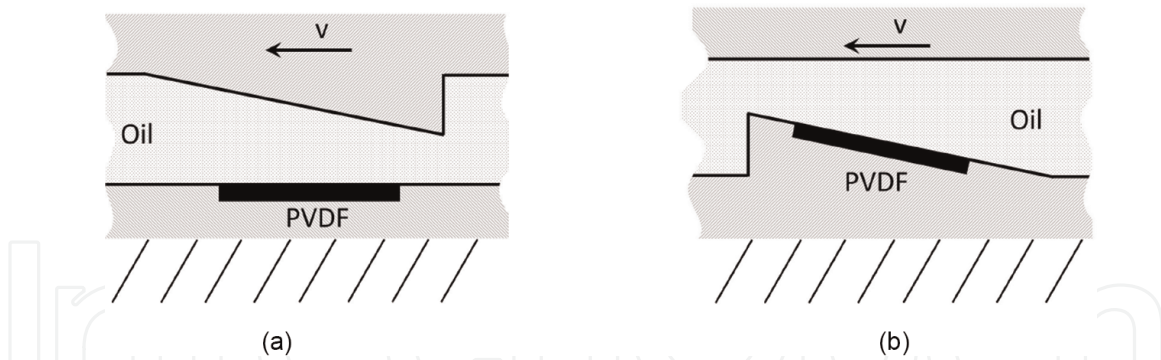
Figure 1.
The arrangement of the PVDF film within the thrust bearing in our previous work [8] (a) and in this work (b). In both arrangements the PVDF is embedded on the stationary body and 'v' indicates rotational direction of the rotating body.

[1, 3, 4], however these are limited as it has been shown that due to large perturbations of the oil film thickness, a nonlinear response is required [5–7]. Therefore measuring the internal hydrodynamic forces inside the thrust bearing is ideal. This paper attempts to address this problem by using intrinsic piezoelectric sensors installed inside the thrust bearing itself. Conventionally this would be done with accelerometers however their physical properties make them unsuitable for use inside a moving bearing. Another option is the use of thin piezoelectric polymer film such as PVDF (Polyvinylidene Fluoride).

In our previous paper [8], an in-depth review of the use of PVDF to measure dynamic forces in static structures [4, 9–16] was discussed. It was noted that PVDF cannot measure absolute pressures, only the fluctuations, which is a common use of PVDF in fluids [17–22], due to its piezoelectric properties [23, 24]. The paper reported on the use of PVDF inside a thrust bearing to measure the pressure fluctuations and infer the change in contact force. Due to limitations in the experimental design, namely the placement of the PVDF films in relation to the pads on the rotating body, the signatures captured from the PVDF films were heavily influenced by the Pad Passing Frequency (PPF). Hence, although that study found that the sensors could measure the pressure fluctuations generated by the sliding pads, the true nature of the excitation of interest, the BPF was masked.

Here, the design of the experiment was reworked so that the true excitation force from the propeller and the resulting change in contact force within the bearing could be observed without the influence of the PPF. This was achieved by placing the PVDF in the tilted portion on the stationary body.

The previous configuration, **Figure 1a**, resulted in the pressure profile generated by the pad sliding over the PVDF film. This led to the dynamic pressure fluctuations being subjected to the PVDF from the pad motion relative to the PVDF sensor. The new configuration proposed in this study (b) removes this component and results in the PVDF film being subjected to the dynamic fluctuations arising from the shaft axial load and hence propeller. The static component of the pad's pressure profile cannot be observed in the signature as a result of the intrinsic nature of PVDF.

2. Materials and methods

The original rig [8], shown in **Figure 2**, is used here and its main attributes described here for completeness. It was designed to model a typical propulsion system
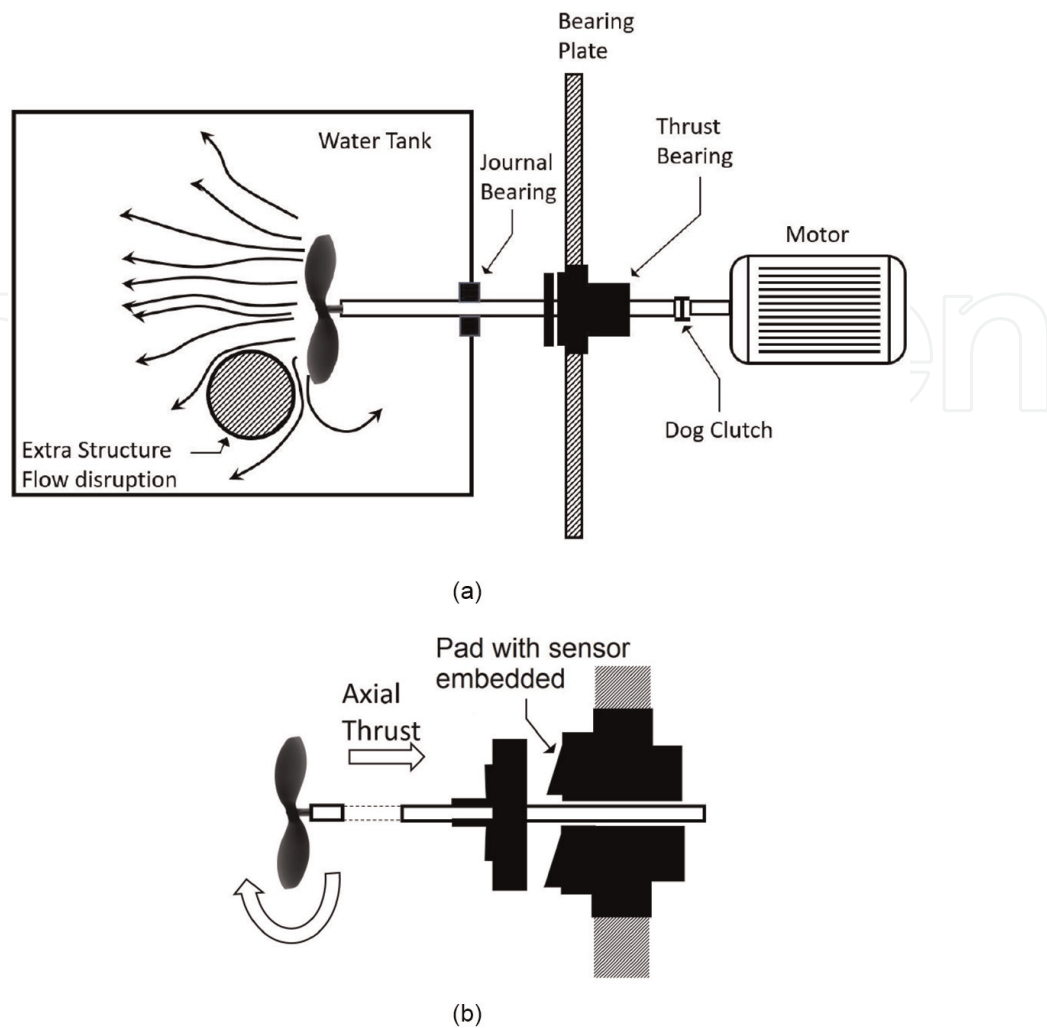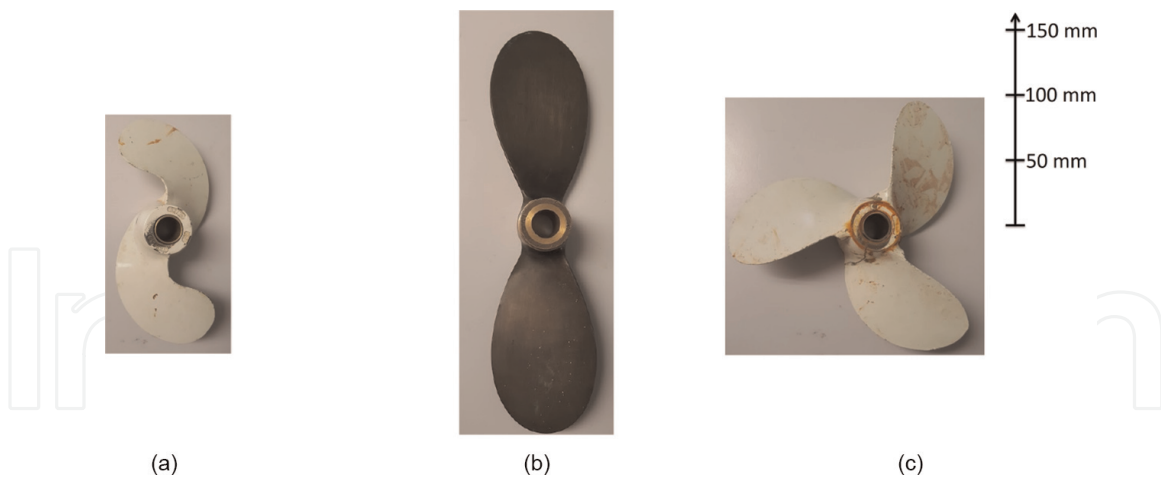
Figure 2.
Schematics of the experimental set-up: (a) layout of entire physical system; (b) enlarged view of propulsion system.

used in marine settings. The system consists of a propeller (prop), shaft, journal bearings, and a thrust bearing attached to a supporting plate structure which represents the hull. The propeller provides axial thrust to the shaft which is transmitted to the hull (supporting plate) via the thrust bearing. The coupling, known as the "dog clutch", is rigid in torsion but flexible in bending thus allowing axial motion to be transmitted along the "floating" shaft. This helps to isolate any unwanted vibration from the motor. The 10 mm thick, 1500 mm wide supporting steel plate is fixed to a concrete block to take the thrust load generated by the propeller and also supports the motor as shown.

A two-blade and three-blade propeller of equal diameter (0.22 m), shown in **Figure 3**, were separately coupled to the propulsion system in the water tank (0.99×0.59×0.58 m) to observe different blade passing forces. A larger (diam = 0.3 m) alternative style bronze two-blade propeller was also used, **Figure 3**.

In addition to the four test configurations (No prop = NP, standard two-blade prop = TBP, bronze two-blade prop = TBBP and three-blade prop = ThBP), two PVDF arrangements were investigated with these test configurations. For each case, the non-rotating component into which the PVDF was embedded was constructed out of ABS (Acrylonitrile Butadiene Styrene) using a 3D printer. Since the forces, temperatures and operating times were relatively low, it was presumed that using the plastic

Figure 3.
Propellers used in the experiment: (a) standard two-blade; (b) bronze two-blade; and, (c) three-blade.

material inside a functioning, small-scale, thrust bearing would not be a problem. This was confirmed by our previous study [8].

Two different designs were investigated regarding the placement of the PVDF: Case 1 - the stationary component was a plain washer with the thrust washer in the rotating component sliding over top as in our first study [8]; Case 2 - was arranged such that the stationary component had the thrust washer and the PVDF embedded on top, with a plain washer in the rotating component sliding over top. Both arrangements (cases) had the PVDF fixed to the non-rotating body to permit the signals to be measured without the need for telemetry or slip rings, **Figure 4**.

In Case 1, **Figure 4**, where the stationary component was the plain washer, recesses were made in the washer to insert two PVDF films as shown. Opposite the plain washer, a thrust washer, also constructed out of ABS, was used with two pads angled at two degrees to the surface. In Case 2, in **Figure 4**, the thrust washer was printed with two, two-degree tilted pads and the PVDF film was embedded into the tilted portion of the washer. Opposite the thrust washer, a plain washer was used in the rotating component. This configuration better resembles what is seen in a typical thrust bearing in a marine propulsion system.

The PVDF sensors were cut from a sheet of 110 μm thick film obtained from Measurement Specialties. Contacts were made using conductive copper tape on the electrodes and the films were glued using West Systems 105 epoxy resin inside the two recesses in the plastic washer. The PVDF sensors were protected by covering the interacting surface of the washer with a thin layer of epoxy. Heat from a blow torch was briefly applied to the epoxy overlaying the PVDF sensors to remove any small bubbles in the thin layer before it was left to cure. Connectors were then added to the end of the cables from the PVDF sensors such that they could be operated independently.

A Brüel & Kjaer (B&K) 2635 charge amplifier was used to condition the signal from the PVDF film. In conjunction with the B&K Pulse Time Data Recorder software, a B&K LAN-XI data acquisition system (Type 3050-B-060) was used to analyse and collect data in the time domain from the PVDF. At a sampling rate of 16,384 Hz, any higher frequency noise from the sensors would be collected while retaining manageable file sizes.

The data was post-processed using Matlab. The raw voltage measured from the PVDF film were converted to force via the measured calibration factor as discussed in
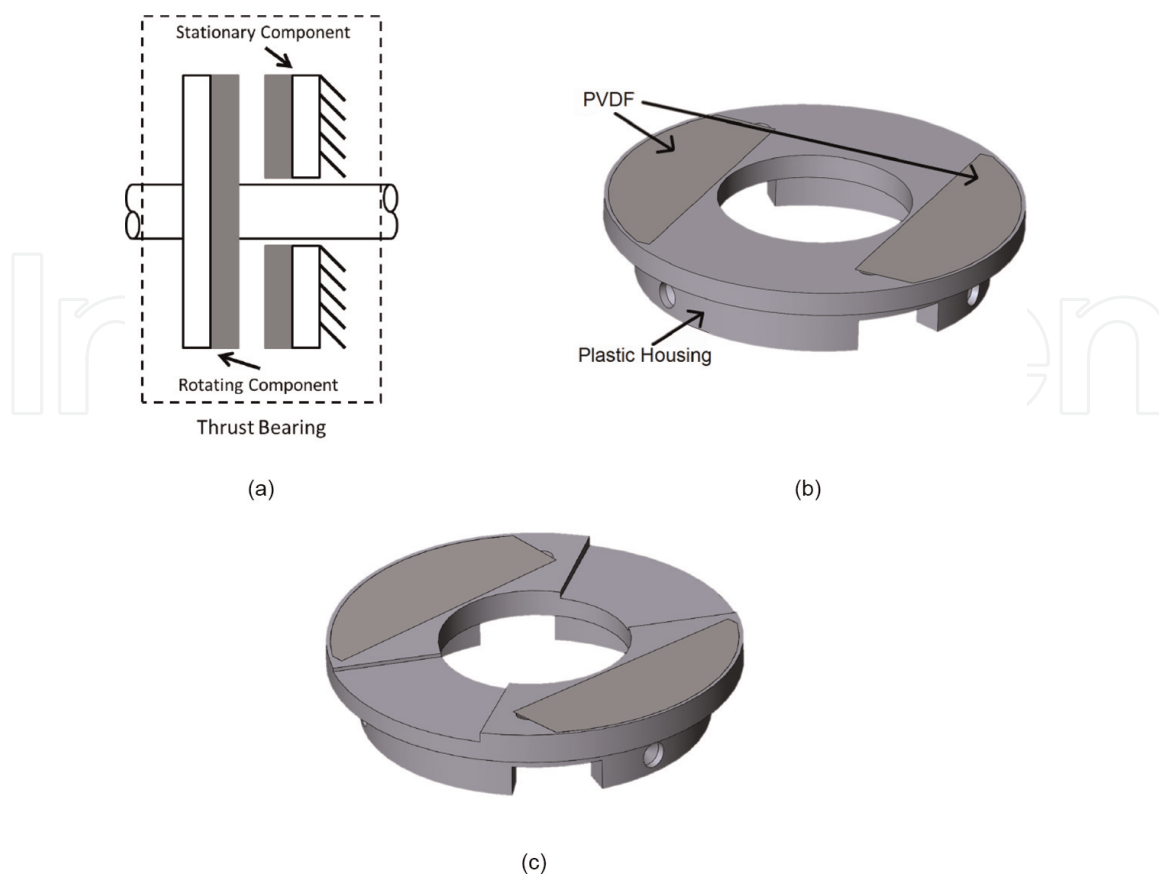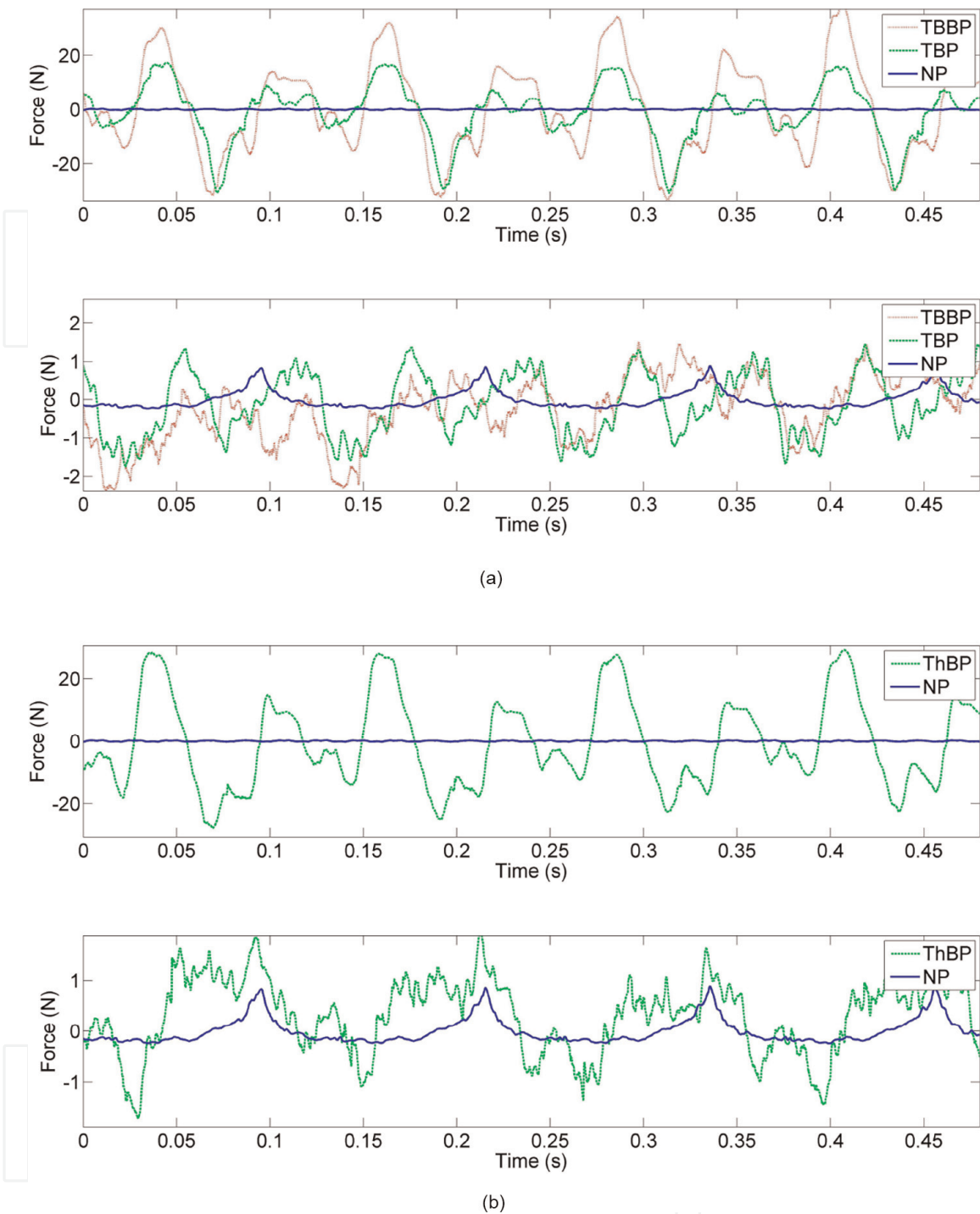
Figure 4.
Thrust bearing comprising stationary and rotation components (a). Stationary bearing configuration: Case 1 -
PVDF embedded in plain washer (b) and Case 2 - PVDF embedded in thrust washer (c).

our previous papers [8, 25]. Although no physical trigger was implemented in the experimental setup, the time domain signals were aligned using Matlab's "alignsignals" function. The frequency-domain data was obtained using the inbuilt FFT function by dividing each track into 8 equal segments to obtain a better frequency representation of each time-domain signal. Each segment was windowed with a Hamming window, with 50% overlap to reduce the effect of windowing.

The set-up enabled the prop shaft to be spun in different configurations. The first being with no propeller at the end of the shaft to give a representation of the noise transmitted to the sensors from just the shaft spinning. Then, three different propellers were attached to the shaft in turn and rotated at speeds of 0 to 600 RPM in 20 RPM increments. Each configuration was performed for both Case 1's and 2's design.

3. Results and discussion

Figures 5 and **6a** shows the results with Case 1 bearing arrangement at 500 RPM for each of the three aforementioned propellers. The features seen here are representative of what is discussed in our previous paper [8]. **Figures 5** and **6b** show the result when the bearing design of Case 1 (**Figure 4**) is replaced with Case 2 (**Figure 4**). The result pertains to the force from one of the embedded sensors at 500 RPM, the other channel shows similar trends. In this arrangement, the sensor signature is dominated by the blade passing effects.

Figure 5.
Time data of the captured dynamic force from the PVDF with Case 1's design (a) and Case 2's design (b). The two (TBP), bronze two (TBBP) and three (ThBP) blade propeller is spun at 500 RPM when compared to no propeller (NP).

The time-domain signatures in **Figure 5** is difficult to interpret due to superposition of the frequency components contained in the signal, however, it can be seen that the propeller force varies approximately ±2 N in Case 2's result. This change in propeller force is similar in magnitude for the three propeller types. In addition to this, the plain shaft exhibits a large signature at the shaft rate, which is attributed to the shaft rotating in the journal bearing which is coupled to the PVDF film via the thrust bearing.

It can be seen in the frequency domain of **Figure 6** that the most significant peak after the shaft rate $\left(A_{f1\ Case\ 2}\right)$ is the second harmonic $\left(A_{f2\ Case\ 2}\right)$ for the two-blade
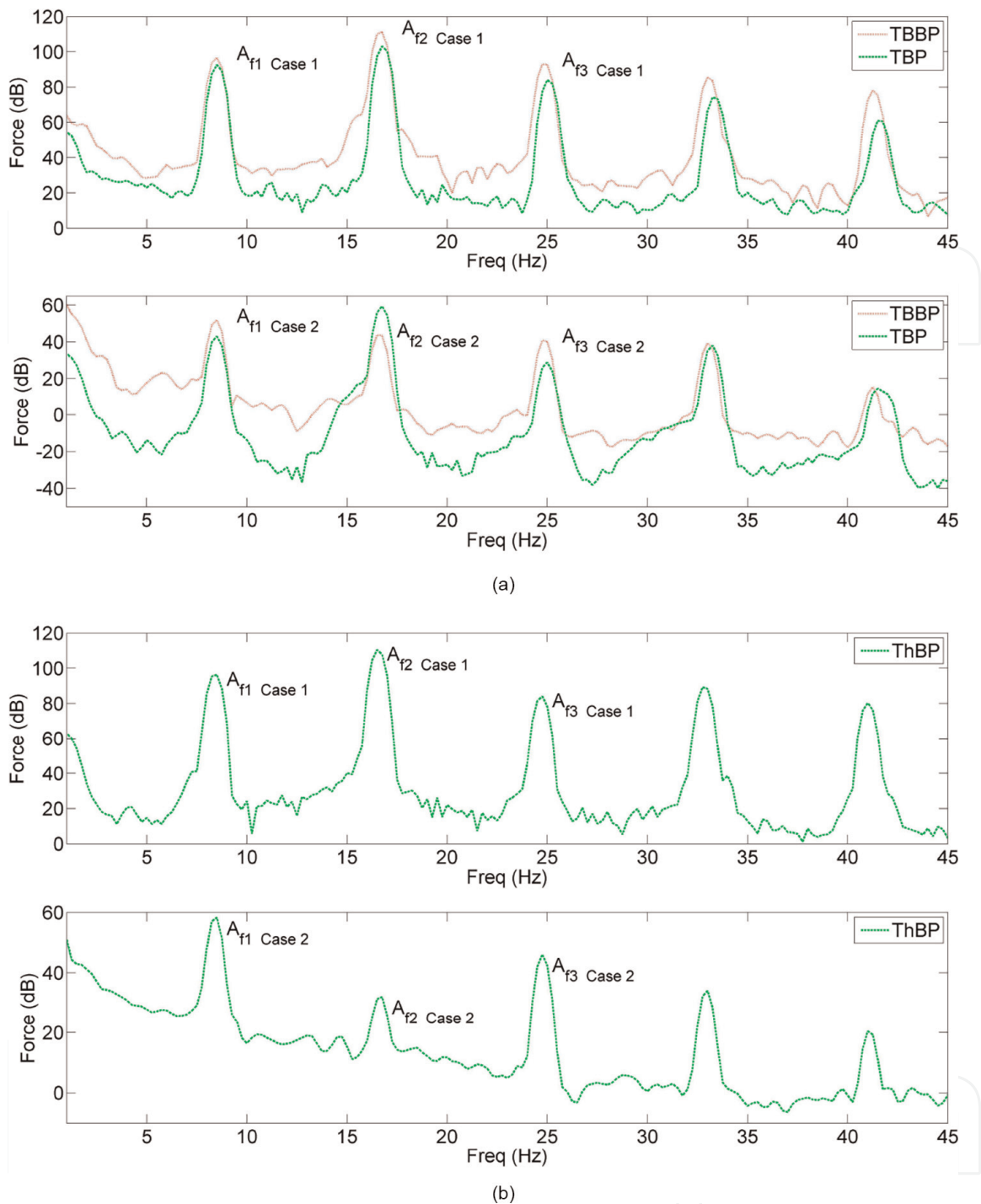
Figure 6.
Frequency data of the captured dynamic force from the PVDF with Case 1's design (a) and Case 2's design (b). The two (TBP), bronze two (TBBP) and three (ThBP) blade propeller is spun at 500 RPM when compared to no propeller used (NP).

result and the third harmonic $\left(A_{f3\ Case\ 2}\right)$ for the three-blade propeller, these correspond to the respective BPFs. The effect of the PPF is eliminated as $A_{f2\ Case\ 2} < < A_{f3\ Case\ 2}$ with reference to the three-blade result; the improvement is less apparent if considering just the form without accounting for the amplitude regarding the two-blade data as the PPF and BBF are superimposed for these arrangements involving a bearing comprising 2 pads and propellers with 2 blades. This is in contrast to when the PVDF is embedded as in Case 1's design. No matter which propeller is

used, the second harmonic of the shaft rate is the most significant,
$A_{f2 \text{ Case } 1} > A_{f3 \text{ Case } 1}$, due to the two pads sliding over the PVDF film. This artefact is a
by-product of the set-up and confounds the true nature of the propeller excitation
forces, as revealed in **Figures 5** and **6** (L2, L4).

These trends can be further demonstrated across all test speeds, and more clearly
depicted in the frequency domain, **Figure 7**. For the plots shown on the left in
Figure 7, 10 s of measured data was recorded for each rotational speed tested. The 10 s
records were stitched together to produce a spectrogram. For clarity, only the three
blade propeller (ThBP) results are shown (similar results were observed for the two
blade propeller variants). The spectrogram amplitudes along the second and third
harmonics have been extracted and are shown in **Figure 7** and denoted by A_{f2} and
A_{f3}, respectively. This method of data representation clearly evidences that the sec-
ond harmonic is typically lower or much closer to the third harmonic for the Case 2
arrangement compared to the Case 1 arrangement.

With reference to the Case 1 results depicted in **Figure 7a**, a bifurcation is
observed about a 50 Hz centre frequency. (This phenomenon was also observed for
the TBP tests not shown here). The bifurcation was not observed in any of the Case 2
tests. The 50 Hz centre frequency is attributed to background Australian supply
voltage EMF. The bifurcation is believed to result from the superposition of the strain
in the PVDF arising from the hydrodynamic force which moves with rotational speed
and the strain caused in the PVDF as a result of it being subjected to the external field.
Further investigation is required to understand this phenomenon.

The proposed PVDF arrangement of Case 2 can also be compared to the initial
PVDF bearing pressure measurement investigation presented by the authors [25]. In
that work the PVDF was embedded in the flat base of the thrust bearing similar to
Case 1's configuration presented herein. The vertical test rig arrangement [25] facili-
tated different rotational speed and different fixed bearing gap investigations in the
absence of a fluid immersed propeller. **Figure 8** shows 300 RPM data from that study
processed into the frequency domain and compares the result to that of the current
study for the Cases 1 and 2 arrangements for the same speed with no propeller (NP).
As the sensitivities of the sensors vary, the data has been normalised to the shaft rate.
There are two attributes: (1) that the second harmonic is reduced when compared
with the original study; (2) that the noise floor is reduced across all frequencies, that
warrant more detailed explanation. Firstly, the results obtained by [25] and Case 1
here show an increase in the second harmonic of the shaft rate when compared to
newly proposed Case 2 arrangement. The larger amplitude pertaining to the original
[25] study compared to Case 1 here is attributed to the increased pressure formed
under the tilted pad as a result of the original set-up which forced a fixed film
thickness whereas in the current study the bearing can adjust the film thickness to
achieve force equilibrium. Secondly, and of potentially greater importance, is that the
noise floor across all speeds has been reduced significantly using the Case 2 arrange-
ment. It is thought that this can be attributed again to the new arrangement's refer-
ence frame. Specifically, that unlike the arrangements that have the pad moving
passed the PVDF, because the PVDF films are mounted on the pads in Case 2 then
they effectively experience the cleaner established pressure field above the pad and
are not as influenced by the frequency content contained in the upstream and down-
stream flow and eddies [25] on each side of the pad. Whilst further experimental and
numerical work is underway, these results add credence to the utility of the new
arrangement.
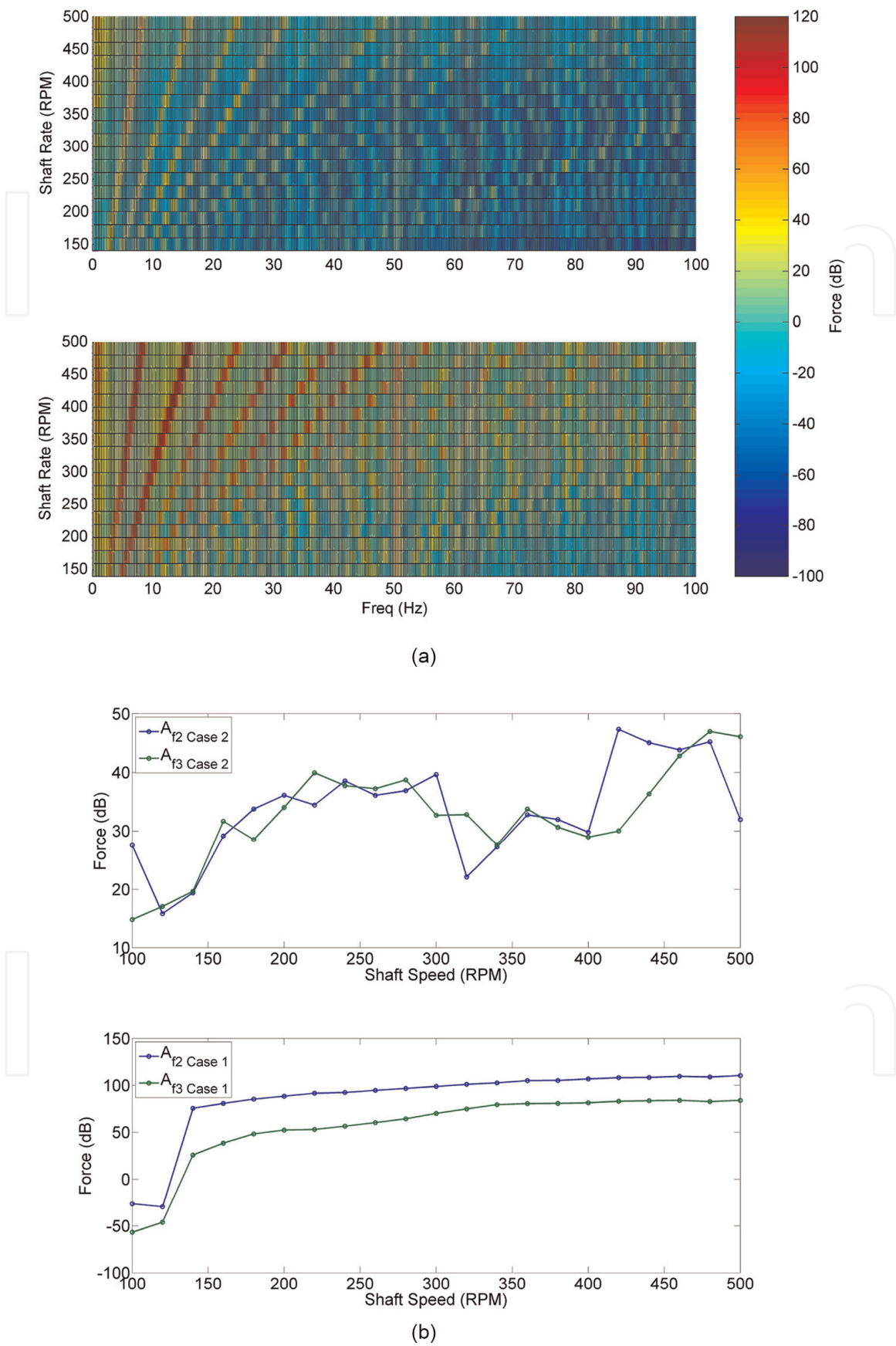
Figure 7.
The frequency response of the PVDF sensors across all test speeds for the Case 2's arrangement and Case 1's arrangement (a) with the three-blade propeller (ThBP). The magnitudes at the second and third harmonics are shown in (b) for both test cases.
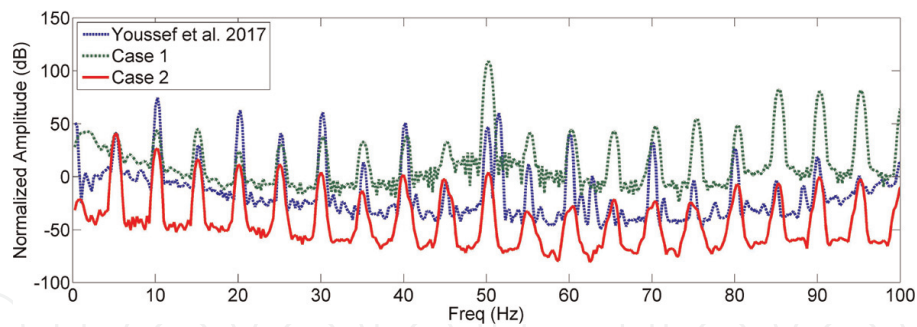
Figure 8.
Comparison of the [25] frequency content to that of Cases 1 and 2 at 300 RPM with no propeller.

4. Summary

The focus of the paper is to evidence differences between results from PVDF sensors when they are placed within different surfaces of the thrust bearing. In particular, the pad passing frequency (PPF) was discovered when the rotating pads act across the surface of the sensors. Also observed was an increase in broadband noise associated with fluid motion generated by the rotating pads. Both of those observations are important for the measurement of the interaction force within a thrust bearing. The PVDF placement on the pad, on the other hand, provides signals free from the pad passing and broadband signals as a result of the changed reference frame. This significant reduction in the noise floor across the full frequency of rotational speeds tested is achieved without post processing filtering. Despite its promise, this latter configuration of the PVDF placement is by no means to be the optimal placement, as the interpretation of the PVDF output in terms of the force components on its surface and the dynamic response of the structure upon which the sensor is attached still require more sophisticated experimental and modelling work.

Conflict of interest

The authors declare no conflict of interest.

Author details

Andrew Youssef[*][†], David Matthews[†], Andrew Guzzomi[†] and Jie Pan[†]
School of Engineering, The University of Western Australia, Perth, Australia

*Address all correspondence to: andrewyoussef22@gmail.com

† These authors contributed equally.

IntechOpen

References

[1] Dylejko PG, Kessissoglou NJ, Tso Y, Norwood CJ. Optimisation of a resonance changer to minimise the vibration transmission in marine vessels. Journal of Sound and Vibration. 2007;**300**(1):101-116

[2] Kingsbury A. Development of the Kingsbury thrust bearing. Mechanical Engineering. 1950;**172**:957-962

[3] Sawicki JT, Rao TVVLN. A nonlinear model for prediction of dynamic coefficients in a hydrodynamic journal bearing. International Journal of Rotating Machinery. 2004;**10**(6): 507-513

[4] Lee I, Sung HJ. Development of an array of pressure sensors with PVDF film. Experiments in Fluids. 1999;**26**(1): 27-35

[5] Pan J, Farag N, Lin T, Juniper R. Propeller induced structural vibration through the thrust bearing. In: Proceedings of the Annual Conference of the Australian Acoustical Society. Adelaide, Australia; 2002. pp. 13-15

[6] Parkins DW, Horner D. Tilting pad journal bearings—Measured and predicted stiffness coefficients. Tribology Transactions. 1993;**36**(3): 359-366

[7] Zhang S, Zhang Q. Coupled torsional and axial nonlinear vibration model of the crankshaft with a propeller. In: 2008 Asia Simulation Conference 7th International Conference on System Simulation and Scientific Computing. Beijing, China: IEEE; 2008. pp. 668-674

[8] Youssef A, Matthews D, Guzzomi A, Pan J. Contact force measurement in an operational thrust bearing using PVDF

film at the blade and pad passing frequencies. Sensors. 2018;**18**(11):3956

[9] Sahaya Grinspan A, Gnanamoorthy R. Impact force of low velocity liquid droplets measured using piezoelectric PVDF film. Colloids and Surfaces A: Physicochemical and Engineering Aspects. 2010;**356**(1):162-168

[10] Kim J, Park Y, Choi I, Kang D. Development of smart elastomeric bearing equipped with PVDF polymer film for monitoring vertical load through the support. VDI Berichte. 2002;**1685**: 135-140

[11] Mahale BP, Bodas D, Gangal SA. Development of PVDF based pressure sensor for low pressure application. In: Nano/Micro Engineered and Molecular Systems (NEMS), 2011 IEEE International Conference on. Kaohsiung, Taiwan: IEEE; 2011. pp. 658-661

[12] Nash BT. Pressure mapping using PVDF film. The UNSW Canberra at ADFA Journal of Undergraduate Engineering Research (Canberra, ACT, Australia). 2012;**4**(1):2-16

[13] Shirinov AV, Schomburg WK. Pressure sensor from a PVDF film. Sensors and Actuators A: Physical. 2008; **142**(1):48-55

[14] Talbot JP. On the performance of base-isolated buildings: A generic model. [PhD thesis], University of Cambridge. 2002

[15] Tiwari R, Lees AW, Friswell MI. Identification of dynamic bearing parameters: A review. Shock and Vibration Digest. 2004;**36**(2):99-124

[16] Zhang J, Wang Y. On the design of intelligent insoles using PVDF film. In:

Piezoelectricity, Acoustic Waves, and Device Applications (SPAWDA), 2016 Symposium on. Xi'an, China: IEEE; 2016. pp. 193-196

[17] Huiliang G, Zuoyong H, Wenjun Y. The self-noise response of a large-planar PVDF hydrophone to turbulent boundary layer pressure fluctuation. Acta Acustica. 1999:02

[18] Li Q, Xing J, Shang D, Wang Y. A flow velocity measurement method based on a PVDF piezoelectric sensor. Sensors. 2019;**19**(7):1657

[19] Zimo L, Dorantes-Gonzalez DJ, Chen K, Yang F, Jin B, Li Y, et al. A four-quadrant PVDF transducer for surface acoustic wave detection. Sensors. 2012;**12**(8):10500-10510

[20] Van Tol D, Jack Hughes W. Underwater PVDF acoustic intensity probe. The Journal of the Acoustical Society of America. 1993;**93**(4): 2273-2273

[21] Wang Y-C, Huang C-H, Lee Y-C, Tsai H-H. Development of a PVDF sensor array for measurement of the impulsive pressure generated by cavitation bubble collapse. Experiments in Fluids. 2006;**41**(3):365-373

[22] Ren-shu YUAN, Shi-qun SUI. Dynamic response of PVDF thin film under pulse pressure. Instrument Technique and Sensor. 2011;**1**(8)

[23] Gusarov B, Gusarova E, Viala B, Gimeno L, Cugat O. PVDF piezoelectric voltage coefficient in situ measurements as a function of applied stress. Journal of Applied Polymer Science. 2016;**133**(14): APP.43248

[24] Kawai H. The piezoelectricity of poly (vinylidene fluoride). Japanese Journal of Applied Physics. 1969;**8**(7):975

[25] Youssef A, Matthews D, Guzzomi A, Pan J. Measurement of pressure fluctuations inside a model thrust bearing using PVDF sensors. Sensors. 2017;**17**(4):878